NASA
Technical
Paper
2265

February 1984

Wave Drag as the Objec Function in Transonic Fighter Wing Optimizati

Pamela S. Phillips

NASA

NASA
Technical
Paper
2265

1984

Wave Drag as the Objective Function in Transonic Fighter Wing Optimization

Pamela S. Phillips

Langley Research Center
Hampton, Virginia

NASA
National Aeronautics
and Space Administration

**Scientific and Technical
Information Office**

1984

INTRODUCTION

Application of three-dimensional design and analysis codes to aircraft design problems has become increasingly important. Reduced development time and costs are the most obvious benefits. Also, these new computational methods may make it possible to design configurations with improved performance, particularly in the transonic speed range. Since three-dimensional transonic inverse codes have not been fully developed, the trial-and-error design process can still be quite lengthy even with good analysis codes. Optimization can be applied to shorten the design cycle.

The purpose of this study is to utilize a three-dimensional transonic analysis method coupled with a numerical optimization procedure to reduce the wave drag of a fighter wing at transonic maneuver conditions. The code used in this study is called PANDORA (Preliminary Automated Numerical Design of Realistic Aircraft). Developed by Aidala (ref. 1), the code combines a three-dimensional transonic analysis method and a numerical optimization procedure. The analysis method is a modified version of Boppe's small disturbance transonic wing-body code (ref. 2), and the optimization procedure is that of Vanderplaats (ref. 3). Wave drag is evaluated through the use of a formula based on the loss in momentum across an isentropic shock. The optimization procedure minimizes wave drag by modifying the wing section contours from root to tip via a wing profile shape function. Wing angle of attack is also allowed to vary during the optimization procedure.

An existing fighter wing was redesigned with the PANDORA code to provide a significant reduction in wave drag at transonic maneuver conditions. This paper discusses this redesign effort and presents results from optimization. Comparisons between the trends in the airfoil modifications produced by the optimization procedure and those that resulted previously from applying various transonic analysis codes are also presented.

SYMBOLS

AR	aspect ratio
b	wing span
$C_{D,i}$	wing induced drag coefficient
$C_{D,p}$	wing pressure drag coefficient
C_L	total configuration lift coefficient
C_p	pressure coefficient
c	local chord
c_{av}	wing average chord
$c_{d,p}$	wing section pressure drag coefficient
E	Oswald efficiency factor

p	local pressure
t/2c	half-thickness ratio
u	local streamwise velocity component
x	streamwise direction
x/c	chord fraction
y	spanwise direction
z	vertical direction
z/c	camber line
$\Delta z/c$	change in camber line
η	wing span station, 2y/b
ρ	density
ϕ	perturbation velocity potential

DISCUSSION

Transonic Analysis Method

The PANDORA code used in this study was developed by Aidala (ref. 1) and consists of a three-dimensional transonic analysis method coupled with a numerical optimization procedure. The analysis method is essentially Boppe's wing-body code (ref. 2) modified to include the capability of modeling a canard. The governing potential flow equation used in the analysis code is in an extended small-disturbance form. Extra terms have been added to improve the resolution of swept shock waves and to obtain a better approximation of the critical velocity. The flow solution is obtained in a multiple embedded grid system using successive line overrelaxation. The grid scheme and solution process are described briefly. References 1 and 2 provide more detailed information.

The computational space used in the embedded grid scheme consists of a crude Cartesian mesh and embedded fine grids (fig. 1). The physical domain whose boundaries correspond to infinity is transformed to the computational domain with finite boundaries. At the bounding planes, the potential is set to zero except at the downstream and symmetry planes. The flow-field potential is obtained at the downstream plane from the equation

$$\phi_{yy} + \phi_{zz} = 0$$

At the symmetry plane, the conditions

$$\phi_y = 0$$

$$\phi_{xy} = 0$$

are applied.

A secondary mesh system consisting of individual fine grid arrays for the wing and canard is embedded in the crude grid. The fine grid system is sheared and tapered to fit the wing and canard planforms. Wing and canard fine grid arrays are located where crude streamwise mesh planes intersect the planforms. These fine grids are evenly spaced in the vertical and spanwise directions.

The crude and the fine grid solutions interact by alternately updating the solution on the crude and fine grids. Initially, calculations are made only on the crude grid in order to develop the global characteristics of the flow field. The interaction scheme then proceeds by updating the potentials on the perimeter of the fine grids with potentials determined by the previous crude grid solution. Similarly, the crude grid potentials on the lifting surface are determined by the previous fine grid solutions. This interaction process continues until the solution has converged sufficiently.

Output from the analysis code consists of pressure coefficients, convergence history, spanwise load, moment and drag distributions, and total configuration force and moment coefficients.

Optimization Procedure

Through a series of subroutines, the analysis method is coupled with the optimization procedure CONMIN developed by Vanderplaats (ref. 3). This procedure is structured to solve linear and nonlinear constrained minimization problems by a modified method of feasible directions. The design task presented in this paper serves as an example demonstrating the optimization process. Reference 3 provides more detailed information.

The current design task attempts to minimize wave drag at a specific lift coefficient. In optimization terminology, wave drag is the objective function, and the lift coefficient is the lower bound constraint. A set of independent design variables are defined such that they control the shape of the wing surface contour and the wing angle of attack. The optimization process is provided with reference values for the objective function and constraint by the analysis method. These reference values are used throughout the optimization process as discussed below.

The optimization process begins with the sequential perturbation of each design variable by 10 percent to determine the effects on wave drag (objective function) and lift (constrained variable). These effects are based on the changes in the objective function and constrained variable relative to their reference values. From this information, the gradients of both the objective function and constrained variable are calculated with respect to the design variables. With these gradients, a search direction is determined, based on superposition, which will reduce the objective

function if there is no adverse interaction between the variables. After a search direction is determined, the design variables are incremented (stepped) accordingly. For clarity, this portion of the optimization procedure will be referred to as step 1.

In step 2, the process returns to the analysis code with the incremented design variables to calculate the resulting values of the objective function and constrained variable. A comparison is then made between these new values and the reference values (step 3). If the objective function increased or the constraint has been violated, the step size in the search direction is decreased and the process returns to step 2. If the objective function decreased without violating the constraint, the design variables are incremented, and steps 2 and 3 are repeated. When the objective function can no longer be reduced without violating the constraint, optimization is terminated, and a local optimum is assumed to have been found. This constitutes one optimization iteration. The user may specify more optimization iterations, in which case the gradients would be recalculated to determine a new search direction.

For the wave-drag-minimization problem presented in this paper, only one optimization iteration was desired; that is, only one search direction was investigated.

It is fundamental to this optimization procedure that a converged analysis solution be obtained prior to initiating optimization. Since the solution for the initial geometry and freestream conditions is the starting solution for all analysis computations performed during optimization, the comparisons described in steps 1 and 3 above are valid if the starting solution is converged. Without this requirement, the values of the objective function and constrained variable produced with incremented design variables could be from a more converged solution than their reference values.

During the study, a problem of slow convergence of the analysis solution arose as a result of high loading at the wing tip. To overcome this problem, a separate analysis run was used to determine the reference values of the objective function and constraint. The number of iterations for the reference analysis run was determined by the total number of iterations used to develop the solution for the perturbed geometry. As a result, valid comparisons were made between the initial geometry and the perturbed geometry without satisfying the convergence requirement. It should be noted that initially it was believed that only the reference value for the objective function needed to be determined in this manner. This procedure also permitted comparisons between the initial and optimized wing contours at the same time step in the convergence history.

Wave Drag Computation

The wave drag coefficient is calculated in the original version of PANDORA by subtraction of the induced drag coefficient from the wing drag coefficient. The wing drag coefficient is calculated by integration of the section drag coefficient along the span

$$C_{D,p} = \frac{2}{b} \int_0^{b/2} \frac{cc_{d,p}}{c_{av}} \, dy$$

and the induced drag coefficient is obtained from the equation

$$C_{D,i} = \frac{C_L^2}{\pi(AR)E}$$

In place of this determination of wave drag, a more direct computational method was sought that could be used as the objective function for optimization. Steger and Baldwin (ref. 4) have shown that a realistic wave drag quantity can be computed by relating wave drag to the loss in momentum across an isentropic shock. From the relation

$$p_2 + \rho_2 u_2^2 < p_1 + \rho_1 u_1^2$$

where subscript 2 denotes conditions behind a normal shock and subscript 1 denotes conditions in front of a normal shock, an equation for the local wave drag per unit area at a given point on the shock can be derived in terms of the loss in momentum as

$$\Delta d_{wave} = (p_1 + \rho_1 u_1^2) - (p_2 + \rho_2 u_2^2)$$

Note that no account is taken of the shock sweep. Integration of this equation gives local wave drag at each wing span station. The total wave drag coefficient is then obtained through integration and nondimensionalization of the local values across the span.

Implementation of this wave drag computation requires a reliable method to determine the shock location at each wing span station. Two methods were investigated.

The first method determined shock location based on the local flow velocities. The location of the first subsonic point aft of the supersonic zone was used as the shock location. This method has been shown to work for small disturbance treatment of two-dimensional transonic flow in reference 4. However, from figure 2 (method 1), it can be seen that for the present three-dimensional problem there is a significant difference between the onset of the shock and the shock location as determined by this method. These results indicate that the first method is not a reliable indicator of shock location for the present problem.

In the second method, pressure coefficients were calculated at each span station starting from the leading edge and proceeding in the streamwise direction to the first subsonic point aft of the supersonic zone. The gradients of the local pressure coefficients with respect to chord location were then computed. The chord location of the largest pressure gradient was deemed the shock location. Figure 2 (method 2) illustrates the computed shock location obtained with the second method for several span stations. To initiate the wave drag computation at the onset of the shock, it was necessary to begin calculations four mesh spaces (0.04c) upstream of this point.

This was a sufficient amount, since the method consistently selected the second or third mesh point on the shock regardless of shock strength (fig. 2). This method of determining shock location was used in the wave drag procedure.

Wing Geometry/Shape Function

The initial geometry is an early version of the Pathfinder II wing-body fighter configuration (fig. 3) developed at the Langley Research Center (ref. 5). The wing planform has a leading-edge sweep of 45° and a trailing-edge sweep of 11.9°. Aspect ratio is 3.28, and taper ratio is 0.214. An axisymmetric model of the fuselage is used. A second wing design developed from the initial geometry through the use of various transonic analysis codes was used to evaluate the trends of the optimized wing profile shapes. Figure 4 gives the thickness distribution for both wing geometries. The camber lines for the initial wing geometry are given in figure 5, and the differences in camber lines between these two configurations are given in figure 6. It was anticipated that through optimization the wing profile shapes of the initial geometry would be modified such that the trends observed in figure 6 would be produced.

A shape function was constructed such that the entire wing could be optimized in one optimization run. To make the resulting wing more feasible, six variables which allow emphasis on specific areas of the wing where modifications are more important were included in this shape function. The shape function is

$$\Delta z\left(\frac{x}{c},\eta\right) = 4\left[C_2\, A_1(\eta)\, a_1 + C_3\, A_2(\eta)\, a_2 + C_4\, A_3(\eta)\, a_3\right]\left(\frac{x}{c} - x_o\right)^2 + \left[C_5\, B_1(\eta)\, b_1 + C_6\, B_2(\eta)\, b_2 + C_7\, B_3(\eta)\, b_3\right]\left(\frac{x}{c} - x_o\right)^3$$

where a value of 0.4 was taken for x_o, and Δz represents the change in the camber line. No changes were made to the wing profile shapes forward of 0.4c. The thickness distribution was held fixed so it was not necessary to optimize the lower surface separately. The variables C_2 to C_7 are design variables whose values are determined by the optimization procedure. The coefficients A_1 and B_1 represent wing changes which are largest at the root and decrease to zero at the tip; the coefficients A_2 and B_2 represent wing changes which are uniform from root to tip; and the coefficients A_3 and B_3 represent wing changes which are largest at the tip and decrease to zero at the root. (See table I.) Coefficients A_1 to A_3 and B_1 to B_3 may be "turned on or off" by specifying each coefficient a_1 to a_3 and b_1 to b_3 to be either one or zero, to control the type of wing change allowable.

Two sets of values for the a and b coefficients were constructed for optimization. (See table II.) For variable set 1, only a_2 and b_1 were assigned values of one so that a uniform change would be made across the span with slightly more emphasis on the root sections. Because the remaining a and b coefficients were set to zero, only two design variables were used in the shape function. The effect of variable set 2 was to gradually increase the wing modifications from the root to the tip. Four design variables were used in this shape function.

RESULTS

The starting conditions for the optimization procedure were an angle of attack of 12.6° and a freestream Mach number of 0.85 at a lift coefficient of 0.562. The lower bound constraint on lift was set to this value. As discussed previously, a reference analysis run was used to determine the reference value for wave drag to ensure that comparisons were made at the same time step in the convergence history. The reference value for wave drag coefficient was determined to be 0.0077. One optimization iteration was attempted with 60 crude/fine iterations allowed for each flow solution requested by the optimization procedure. Variable set 1, given in table II, was used for the wing shape function, so that two design variables for wing shape modifications and one design variable for changes in wing angle of attack were employed. This three-design-variable optimization produced a lift coefficient of 0.561 and a wave drag coefficient of 0.0070. The wing angle of attack increased to 12.7°. The optimized wing did lower the wave drag coefficient but not without reducing the lift coefficient. Virtually identical modifications were made across the span because of design variable C_3, which was more influential than C_5 in the shape function. The resulting modifications made to the initial geometry, shown in figure 7, did not reflect the trend that was anticipated. This indicated that more emphasis should be placed on modifying the outboard stations. It also appeared that more than two design variables should be used for the wing shape modifications. Evaluation of the gradients of the objective function and constraint made it apparent that a reference value for the lift coefficient should be determined and used in the same manner as the reference value for the wave drag. Because the lift coefficient had not sufficiently converged prior to this optimization attempt, the efficiency of the search direction may have been reduced.

A second optimization was performed starting from a different set of initial conditions. These conditions were changed to reduce the loading at the wing tip while maintaining a higher lift coefficient. These conditions were an angle of attack of 16° at a freestream Mach number of 0.80. A reference analysis run gave the reference values of 0.0077 for wave drag coefficient and 0.716 for lift coefficient. Variable set 2, given in table II, was constructed such that emphasis would be placed on modifying outboard wing stations and increasing the number of design variables influencing the shape function from two to four. One optimization iteration of the configuration yielded a wave drag coefficient of 0.0081 and a lift coefficient of 0.755. The wing angle of attack was reduced to 15.6°. Figure 8 illustrates the modifications to the wing profiles which reflect the desired trend. Although wave drag increased, there was also an increase in the lift coefficient. Without further modifications to the wing profiles, wave drag could be reduced by lowering the wing angle of attack until the lift coefficient reaches its constraint value. To accomplish wing profile modifications and additional reduction in wing angle of attack through optimization would have required more than one optimization iteration; that is, more than one search direction would have to be interrogated.

Through analysis runs, the lift coefficients of the optimized and initial geometry were matched to determine the optimized angle of attack. To obtain more converged solutions, these analysis runs were allowed to run longer than those previously used. After a total of 560 iterations at the same conditions as the second optimization case, the lift coefficient of the initial geometry was 0.735, and the wave drag coefficient was 0.0100. A lift coefficient of 0.738 for the optimized geometry was obtained by reducing the wing angle of attack to 13°. This resulted in a wave drag coefficient of 0.0040. By matching the lift coefficients, a significant decrease in wave drag was achieved. A comparison of the pressure distributions for the baseline and optimized geometries at the above conditions is shown in figure 9.

The shock strength and leading-edge pressure peaks were significantly reduced across the span. Except in the tip region, the onset of the shock moved aft approximately 0.08c.

CONCLUDING REMARKS

The original computational method for determining wave drag in a three-dimensional transonic analysis method was replaced by a wave drag formula based on the loss in momentum across an isentropic shock. This formula was used as the objective function in an optimization procedure coupled with the analysis method to reduce the wave drag of a fighter wing at transonic maneuver conditions. The optimization procedure minimized wave drag at a specific lift coefficient by modifying the wing section contours defined by a wing profile shape function. Through the use of the three-dimensional transonic analysis code and optimization procedure, a fighter wing was redesigned with a significant reduction in wave drag at transonic maneuver conditions. Leading-edge pressure peaks and shock strength were significantly reduced while maintaining a high lift coefficient.

Although a successful optimization was performed with wave drag as the objective function, the high sensitivity to solution convergence demonstrated by this computation may have reduced the efficiency of the optimization process. Further study is needed to reduce the effects of convergence on the wave drag computation. In addition, shock sweep effects should be included in the computation.

The shape function used by the optimization procedure to modify the wing section contours enabled the optimization procedure to modify all wing section contours in one optimization iteration. However, having this capability does put severe limitations on the optimization process. For the particular case presented here, the types of wing contour modifications necessary to reduce wave drag were produced through the use of this shape function.

Langley Research Center
National Aeronautics and Space Administration
Hampton, VA 23665
December 21, 1983

REFERENCES

1. Aidala, P.: Numerical Aircraft Design Using 3-D Transonic Analysis With Optimization. Volume III, Part 2: User's Guide to Fighter Design Computer Program. AFWAL-TR-81-3091, Volume III, Part 2, U.S. Air Force, Aug. 1981.

2. Boppe, Charles W.: Transonic Flow Field Analysis for Wing-Fuselage Configurations. NASA CR-3243, 1980.

3. Vanderplaats, Garret N.: CONMIN - A Fortran Program for Constrained Function Minimization. User's Manual. NASA TM X-62,282, 1973.

4. Steger, Joseph L.; and Baldwin, Barrett S.: Shock Waves and Drag in the Numerical Calculation of Isentropic Transonic Flow. NASA TN D-6997, 1972.

5. Bradshaw, James F.: Status of NTF Models. Cryogenic Wind Tunnel Models - Design and Fabrication, NASA CP-2262, 1983, pp. 63-70.

TABLE I.- SHAPE FUNCTION COEFFICIENTS

η	A_1	A_2	A_3	B_1	B_2	B_3
0	2/3	1/3	0	2/3	1/3	0
.125	2/3	↓	0	2/3	↓	0
.2	2/3	↓	0	2/3	↓	0
.3	1/3	↓	1/3	1/3	↓	1/3
.5	0	↓	2/3	0	↓	2/3
1.0	0	↓	2/3	0	↓	2/3

TABLE II.- SHAPE FUNCTION CONTROL COEFFICIENTS

Variable set 1	Variable set 2
$a_1 = 0$ $a_2 = 1$ $a_3 = 0$ $b_1 = 1$ $b_2 = 0$ $b_3 = 0$	$a_1 = 0$ $a_2 = 1$ $a_3 = 1$ $b_1 = 0$ $b_2 = 1$ $b_3 = 1$

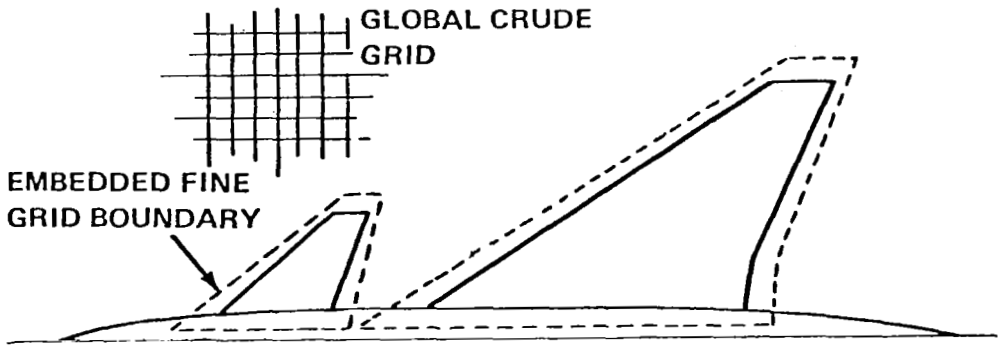

(a) Global crude grid and fine grid boundaries.

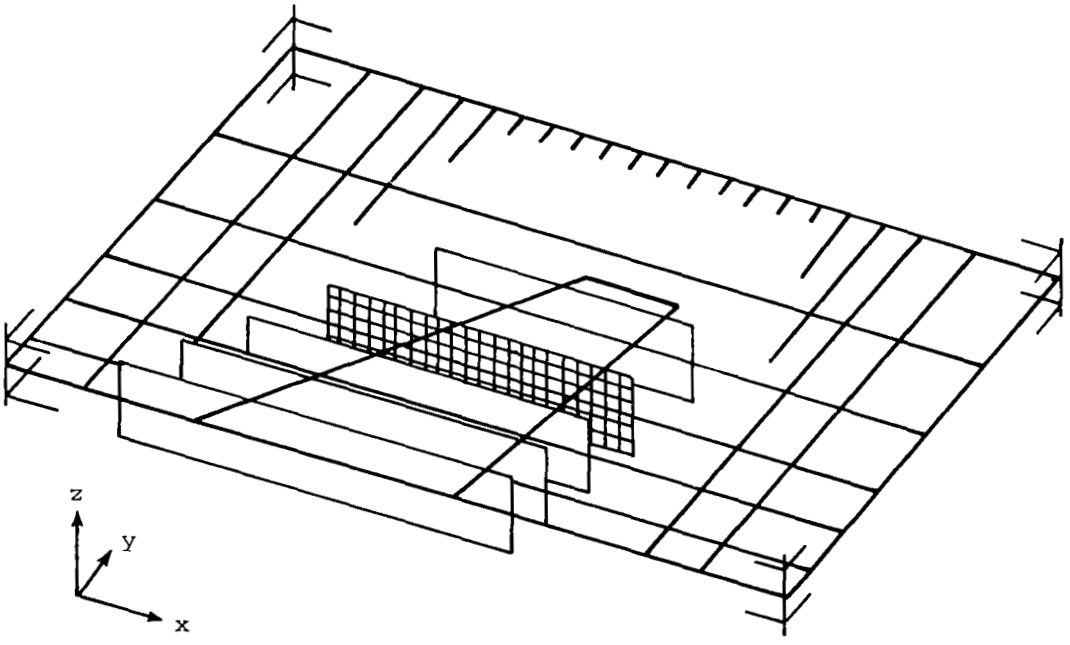

(b) Embedded fine grid system.

Figure 1.- Multiple embedded grid system.

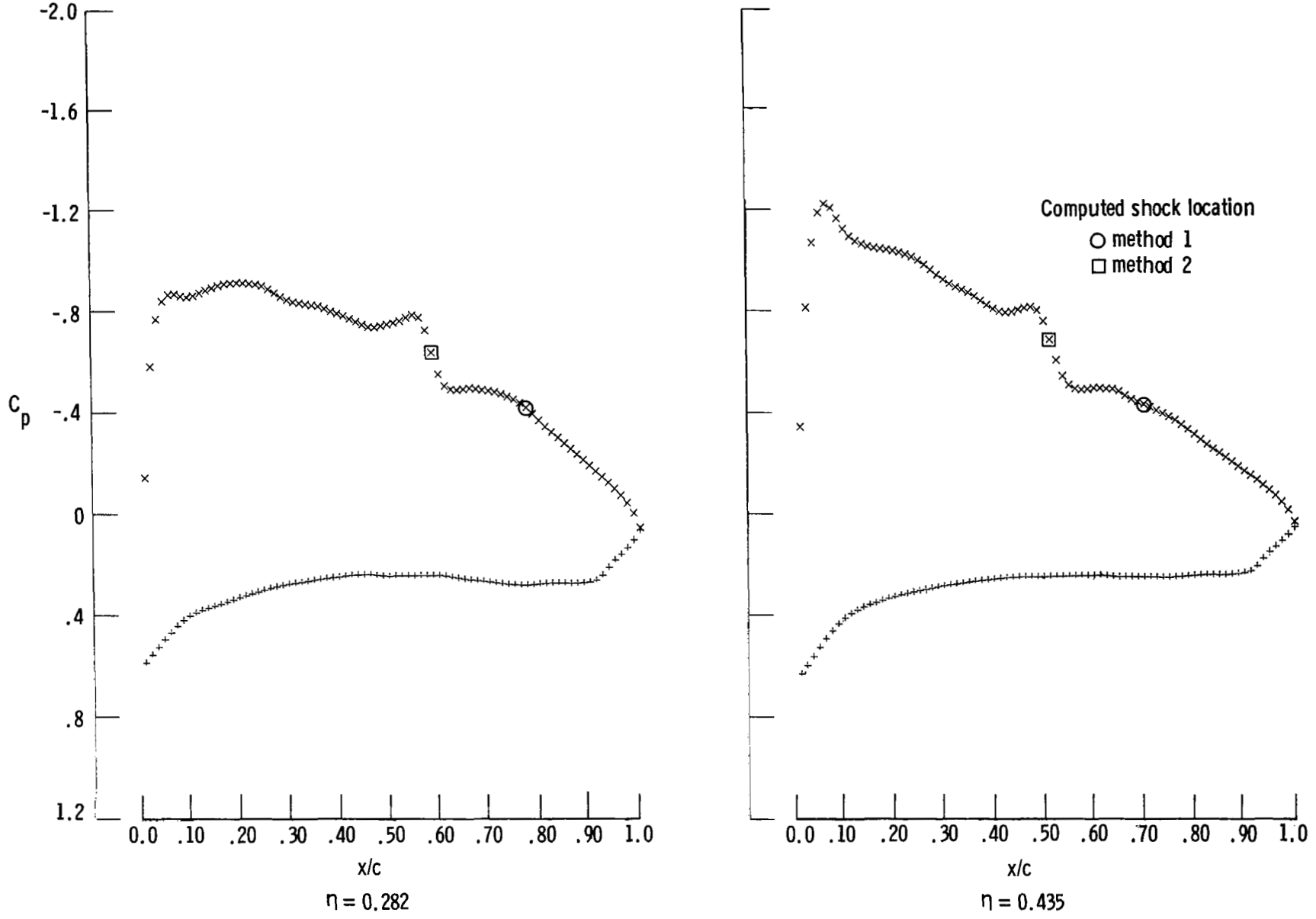

(a) Inboard span stations.

Figure 2.- Comparisons of computed shock locations.

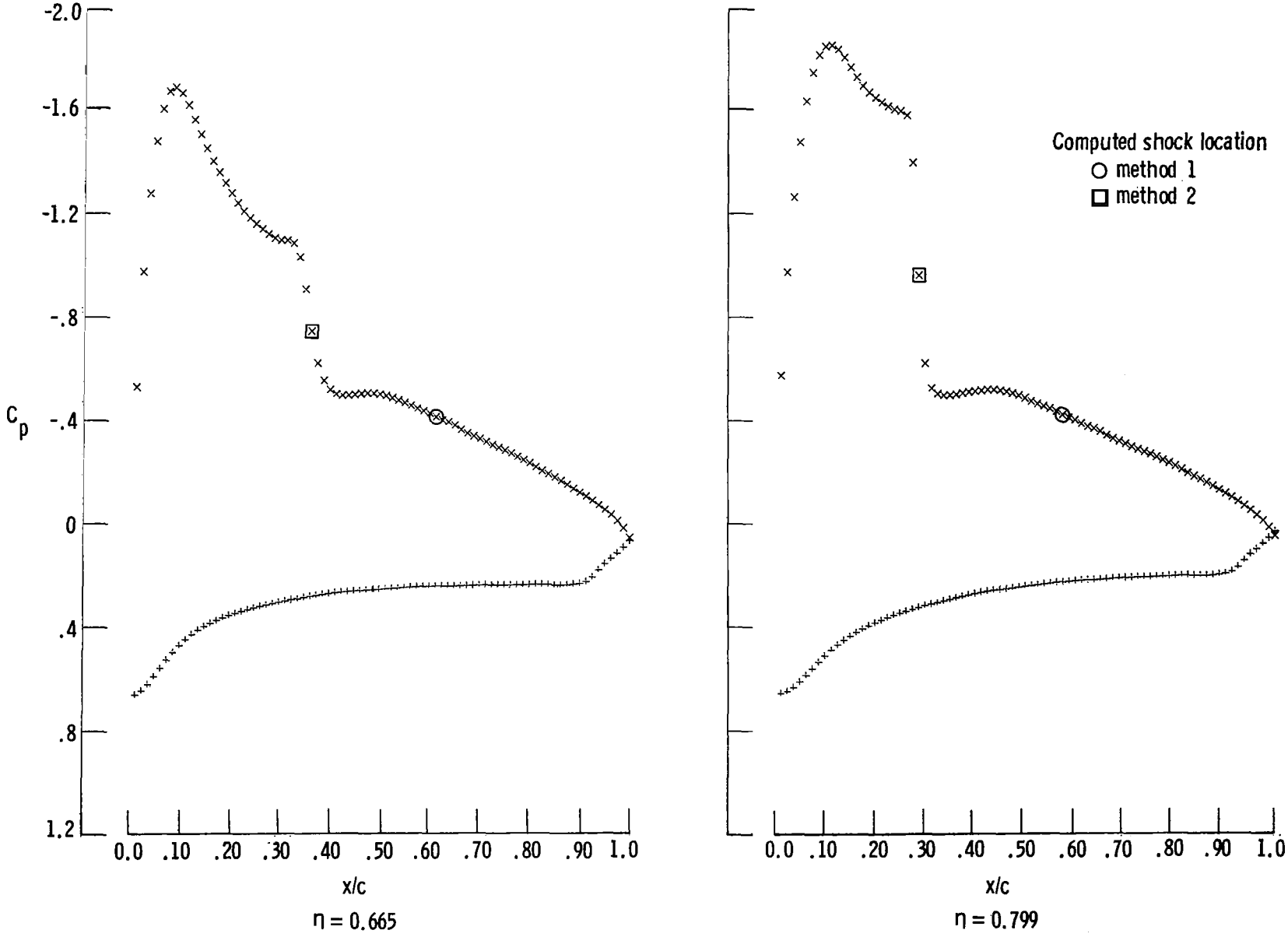

(b) Outboard span stations.

Figure 2.- Concluded.

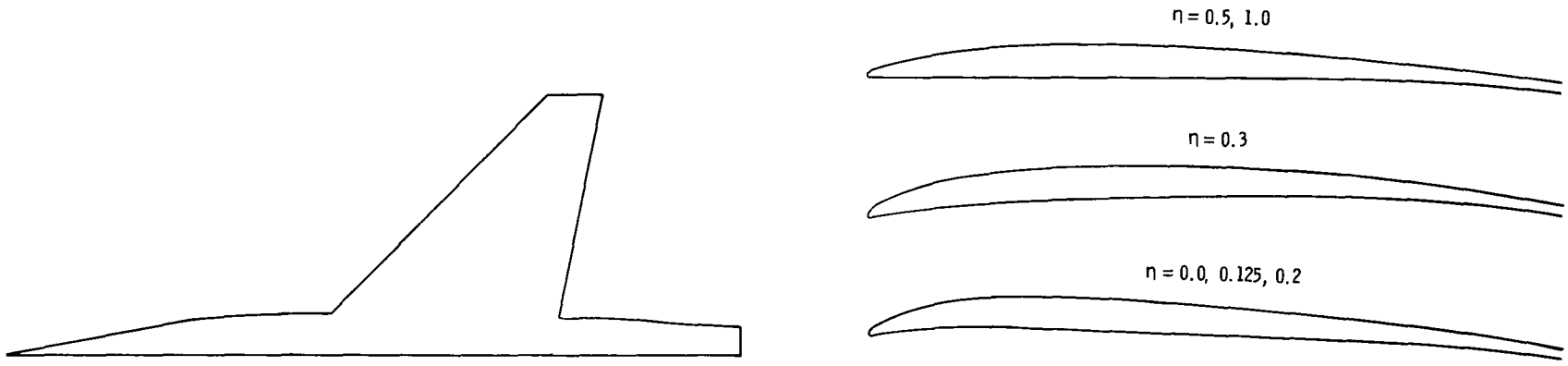

Figure 3.- Wing-body planview and initial airfoil geometry.

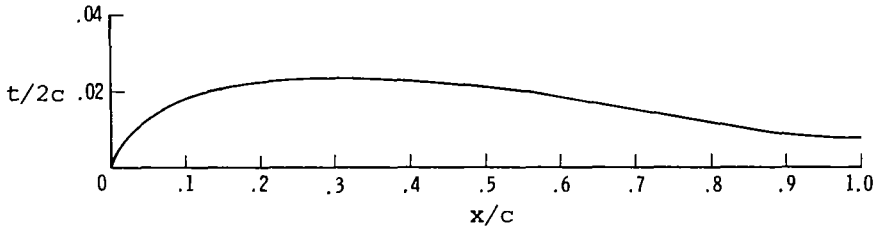

Figure 4.- Half-thickness distribution.

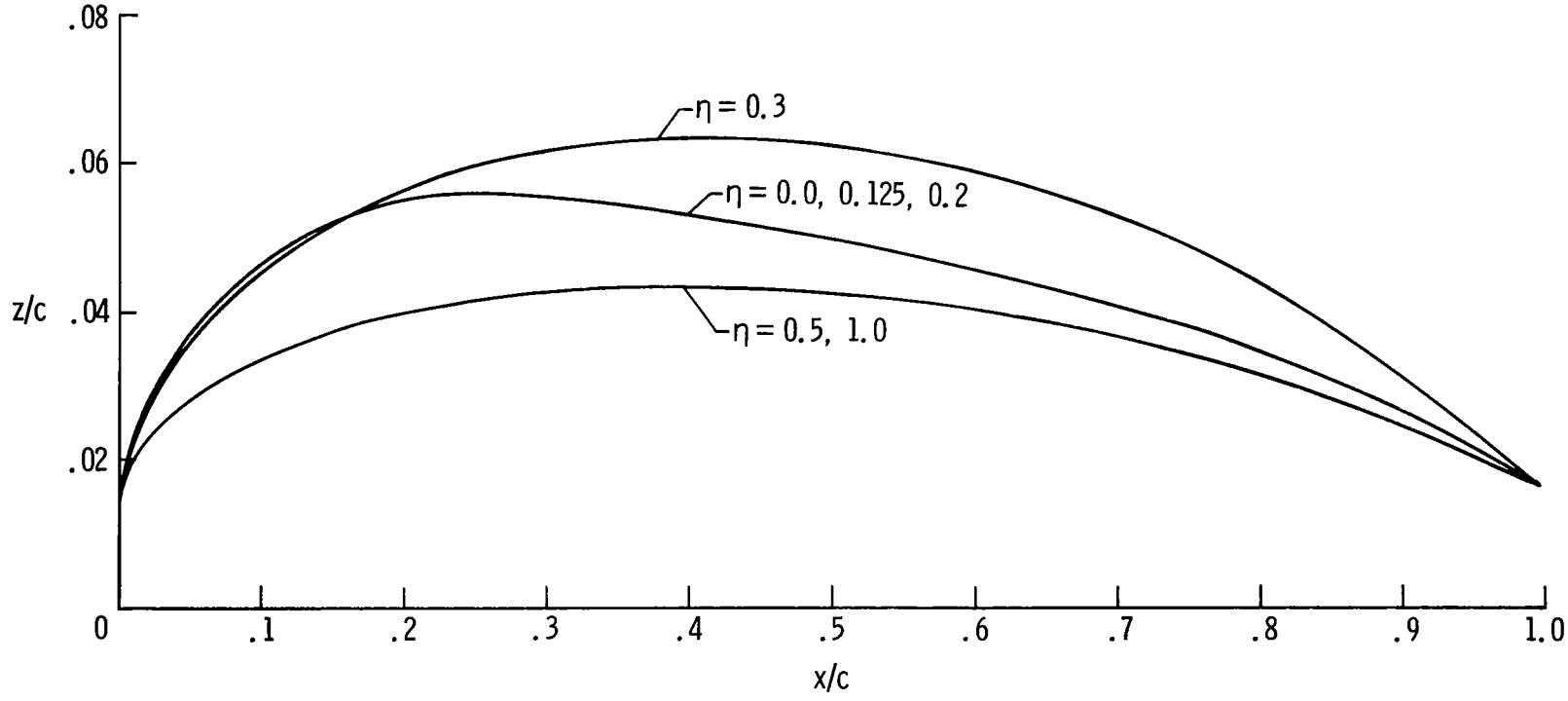

Figure 5.- Camber lines of initial wing geometry.

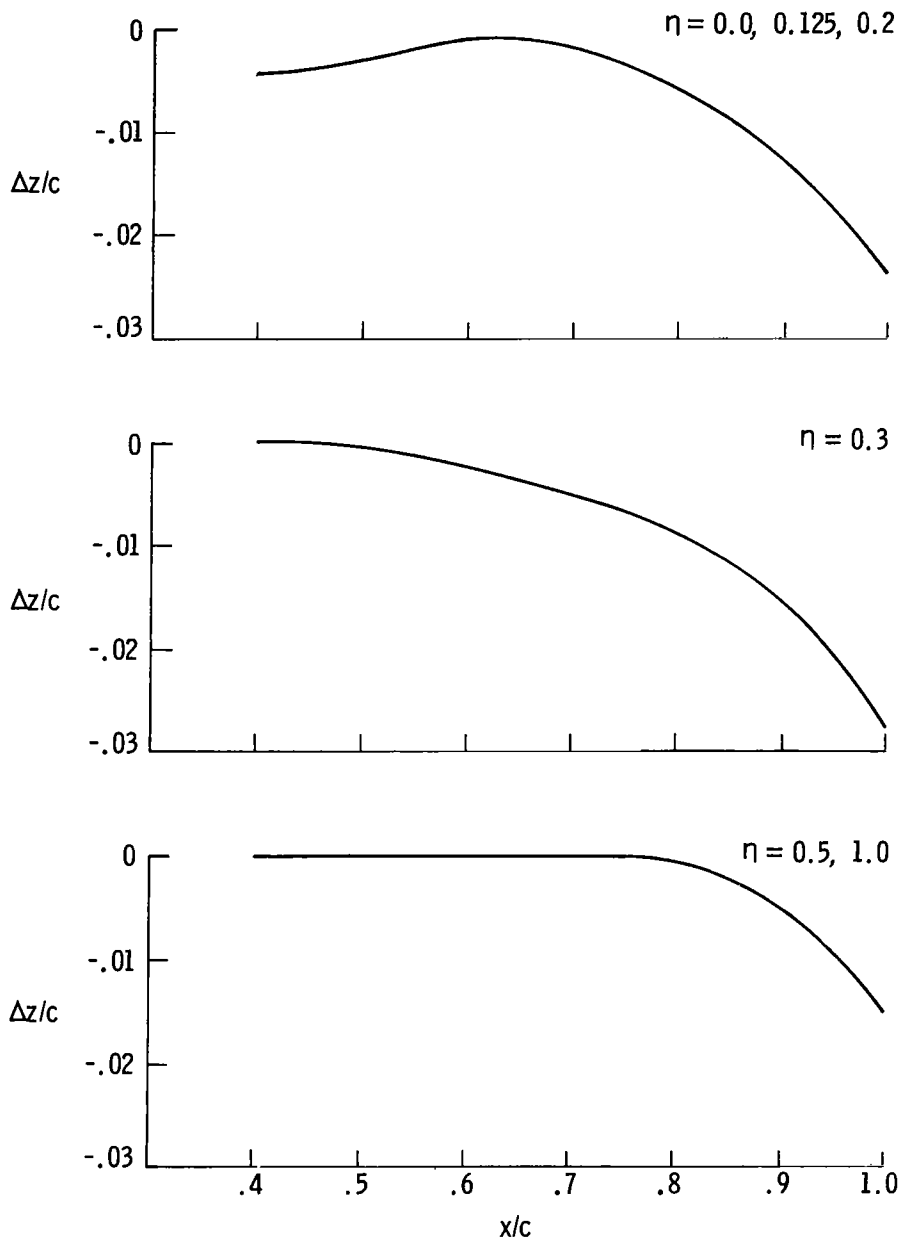

Figure 6.- Camber line differences used to establish wing profile shape trends.

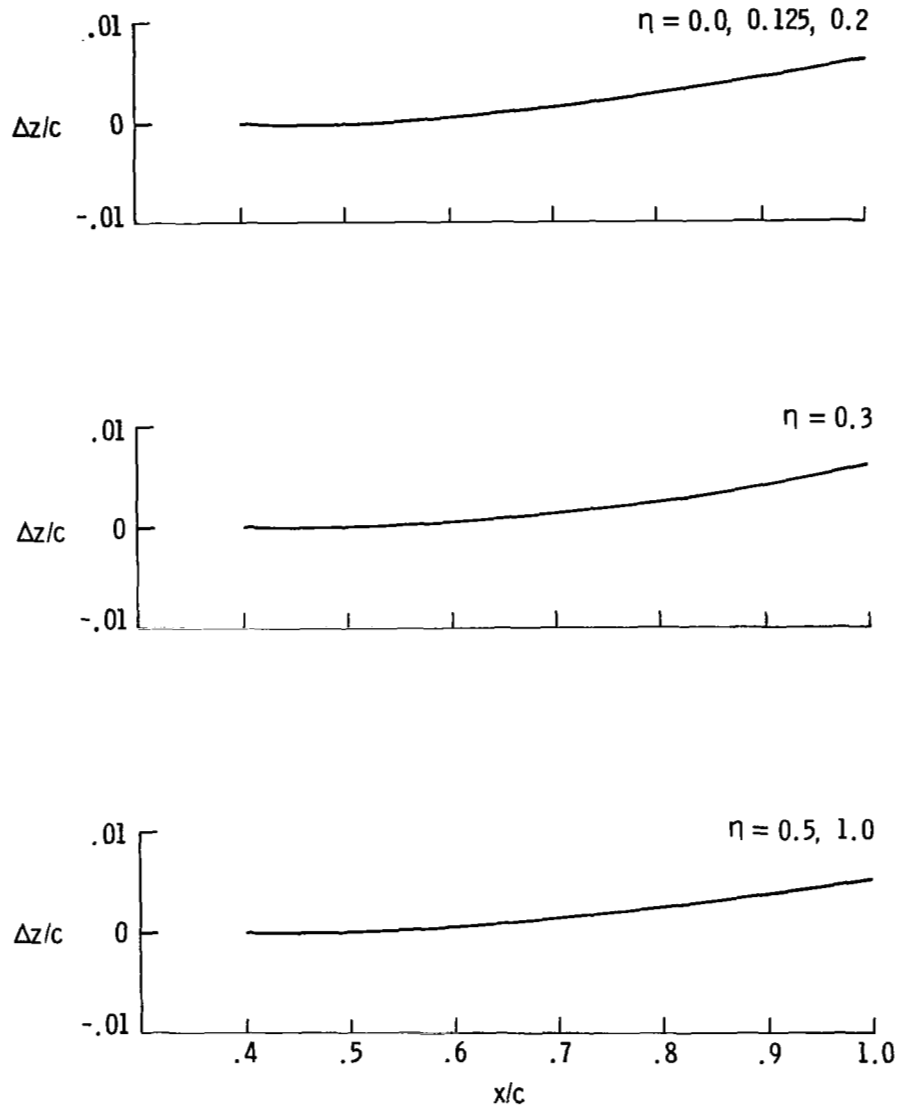

Figure 7.- Camber line modifications to initial wing geometry from the three-design-variable optimization.

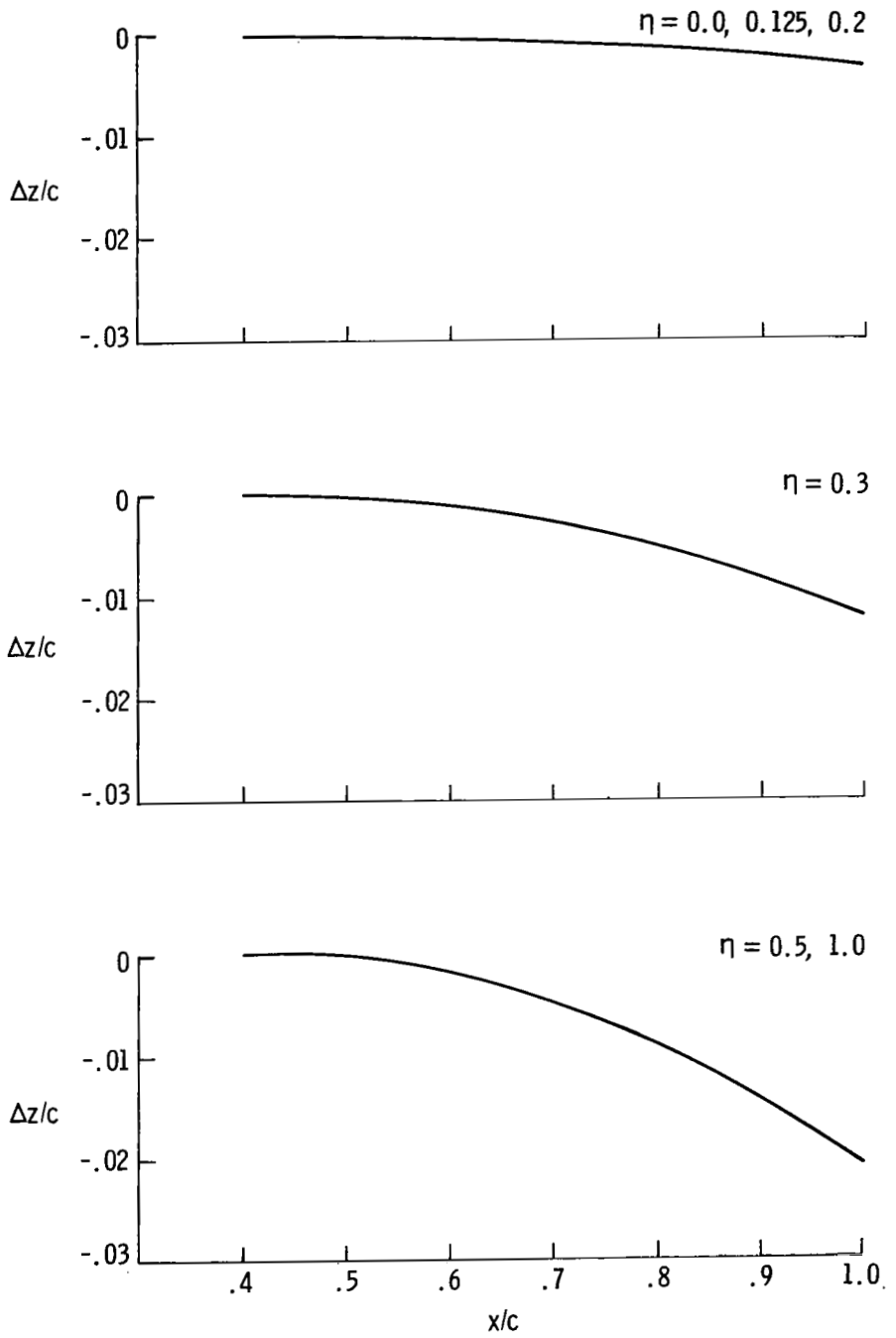

Figure 8.- Camber line modifications to initial wing geometry from the second optimization run.

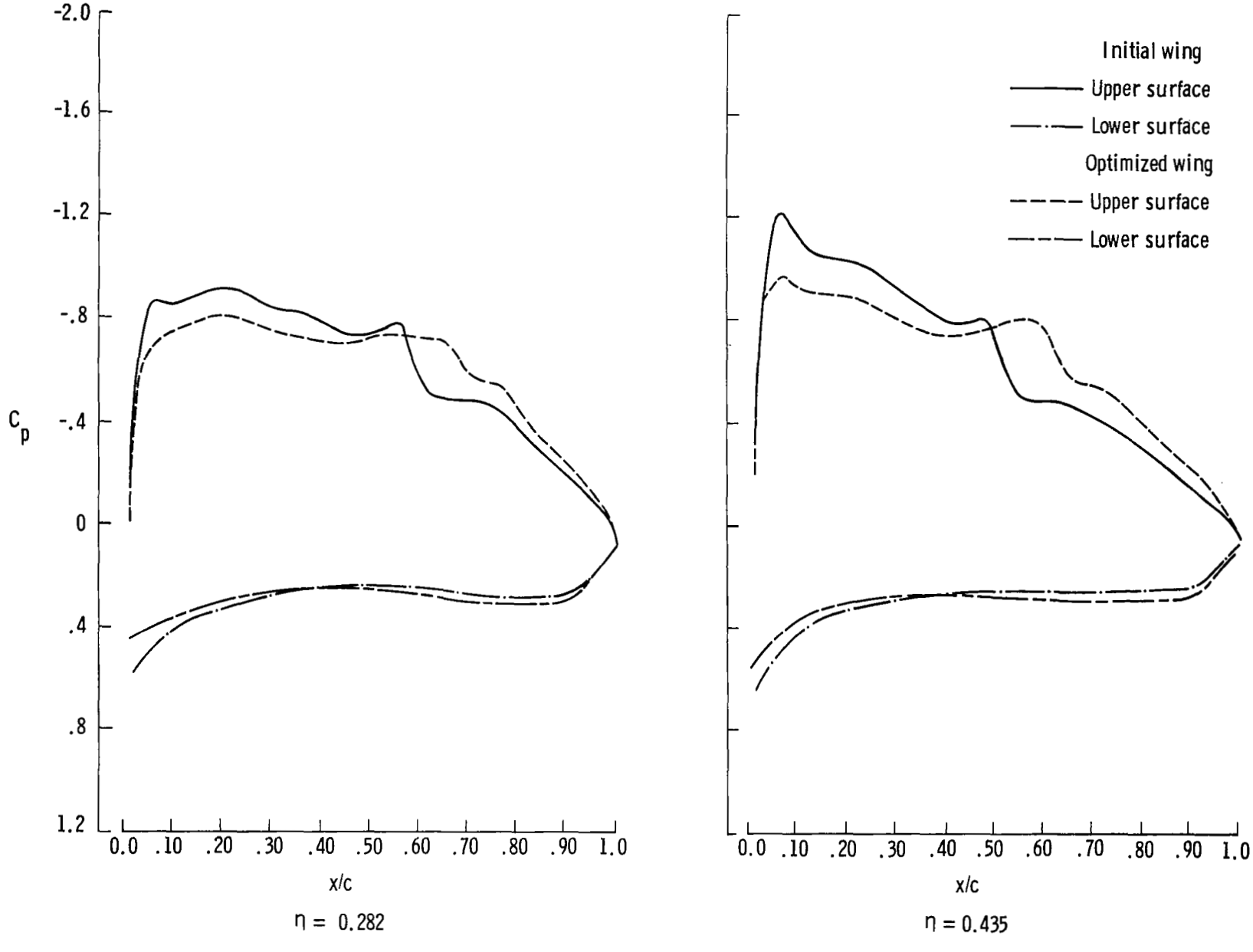

(a) Inboard span stations.

Figure 9.- Pressure distributions for optimized and initial wing geometries.

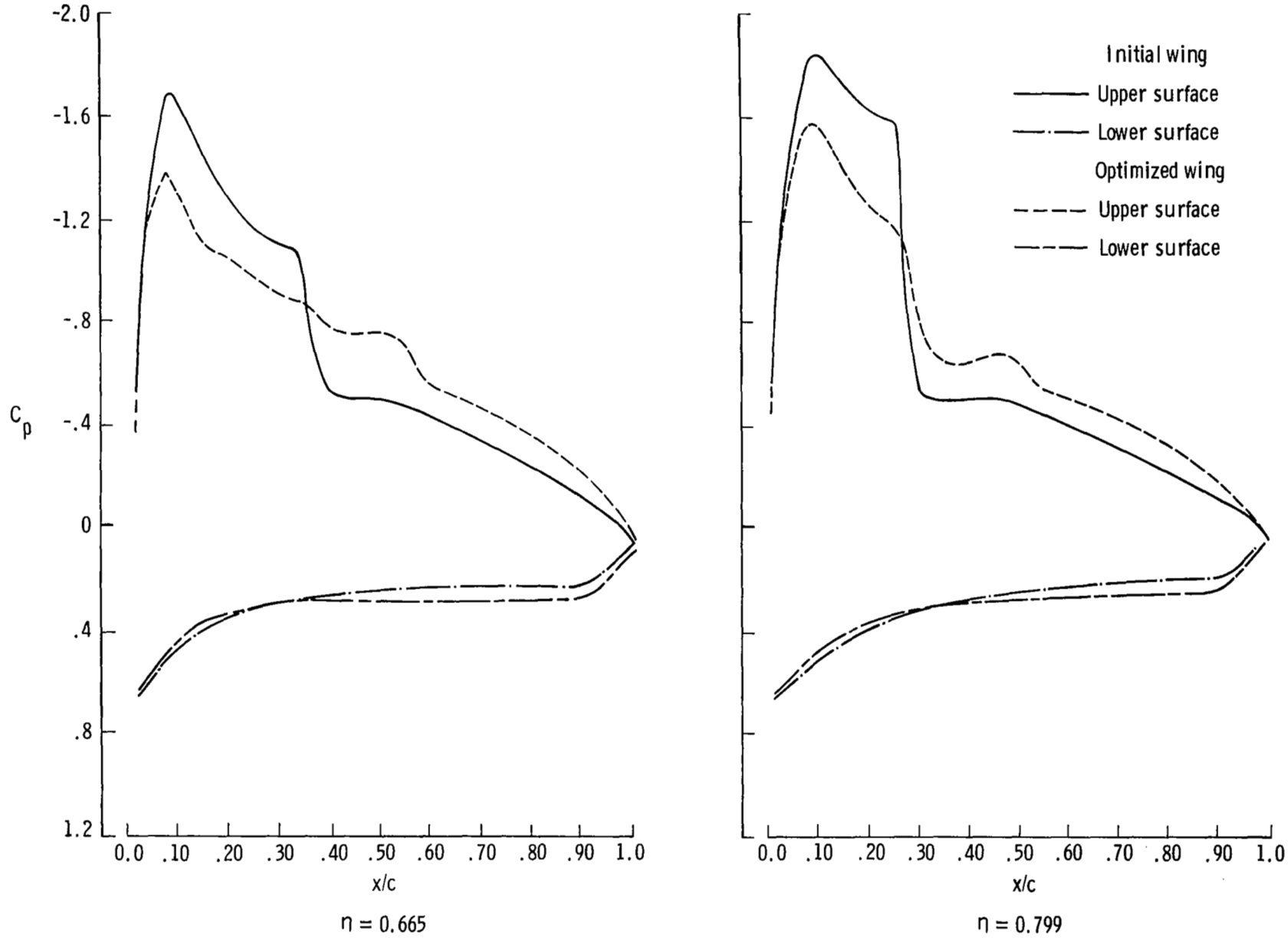

(b) Outboard span stations.

Figure 9.- Concluded.

1. Report No.	2. Government Accession No.	3. Recipient's Catalog No.
NASA TP-2265		

4. Title and Subtitle	5. Report Date
WAVE DRAG AS THE OBJECTIVE FUNCTION IN TRANSONIC FIGHTER WING OPTIMIZATION	February 1984
	6. Performing Organization Code: 505-31-03-01
7. Author(s): Pamela S. Phillips	8. Performing Organization Report No.: L-15687
	10. Work Unit No.
9. Performing Organization Name and Address: NASA Langley Research Center, Hampton, VA 23665	11. Contract or Grant No.
	13. Type of Report and Period Covered: Technical Paper
12. Sponsoring Agency Name and Address: National Aeronautics and Space Administration, Washington, DC 20546	14. Sponsoring Agency Code

15. Supplementary Notes

16. Abstract

The original computational method for determining wave drag in a three-dimensional transonic analysis method was replaced by a wave drag formula based on the loss in momentum across an isentropic shock. This formula was used as the objective function in a numerical optimization procedure to reduce the wave drag of a fighter wing at transonic maneuver conditions. The optimization procedure minimized wave drag through modifications to the wing section contours defined by a wing profile shape function. A significant reduction in wave drag was achieved while maintaining a high lift coefficient. Comparisons of the pressure distributions for the initial and optimized wing geometries showed significant reductions in the leading-edge peaks and shock strength across the span.

17. Key Words (Suggested by Author(s))	18. Distribution Statement
Numerical optimization Wave drag Transonic fighter wing design	Unclassified - Unlimited Subject Category 02

19. Security Classif. (of this report)	20. Security Classif. (of this page)	21. No. of Pages	22. Price
Unclassified	Unclassified	21	A02

For sale by the National Technical Information Service, Springfield, Virginia 22161

NASA-Langley, 1984